GSC Advanced Research and Reviews
eISSN: 2582-4597 CODEN (USA): GARRC2
Cross Ref DOI: 10.30574/gscarr
Journal homepage: https://gsconlinepress.com/journals/gscarr/

(RESEARCH ARTICLE)

Check for updates

Study of the structural, electronic, optical and elastic properties of $NaSrX_3$ (X = F, Cl) perovskite materials using the ab-initio method

Mona Hermann Charly YAPI [1, 2, *], Bakary Coulibaly ABOU [3], Guy Müller Banquet OKRA [1, 2] and Womblegnon Stephane GUIA [1]

[1] *Department of Mathematics Physics Chemistry, Physics Teaching Unit, Laboratory of Environmental Sciences and Technologies, JEAN LOROUGNON GUÉDÉ University, BP 150 Daloa, Côte d'Ivoire.*
[2] *Laboratory of Fundamental and Applied Physics (LFAP), University Nangui Abrogoua, BP 801 Abidjan 02, Côte d'Ivoire.*
[3] *Institute for Research on New Energies, (IRNE), University Nangui Abrogoua, BP 801 Abidjan 02, Côte d'Ivoire.*

GSC Advanced Research and Reviews, 2025, 24(03), 210-224

Publication history: Received on 10 August 2025; revised on 16 September 2025; accepted on 19 September 2025

Article DOI: https://doi.org/10.30574/gscarr.2025.24.3.0287

Abstract

In this work, we studied the structural, electronic, optical, and elastic properties of $NaSrX_3$ type perovskites (X: halogen F and Cl) using density functional theory (DFT) implemented in Quantum-expresso by GGA. The lattice parameters of $NaSrF_3$ and $NaSrCl_3$ are 4.01 Å and 4.65 Å, respectively. We discovered that $NaSrF_3$ behaves as an insulator, while $NaSrCl_3$ behaves as a semiconductor. They have direct gaps. The gap for $NaSrF_3$ is 6.02 eV and that for $NaSrCl_3$ is 4.09 eV. They all have a conduction band dominated by Sr 3d states, weakly mixed with Na 3s and Sr 4s states. The valence band is dominated by alkali 2p and Sr 3d states. These perovskites also have very good optical properties: low reflectivity and high absorption in the ultraviolet range. These materials are elastically stable. They have good rigidity and show greater resistance to bond bending and bond angle distortion. However, $NaSrF_3$ is ductile and $NaSrCl_3$ is brittle. $NaSrCl_3$ will withstand higher temperatures than $NaSrF_3$. This study shows that these materials are suitable for various applications in both the visible and UV ranges. They have very interesting properties for optoelectronics.

Keywords: $NaSrX_3$ perovskites; Solar cell; DFT; Electronic properties; Optical properties

1. Introduction

The world today is experiencing a significant decline in energy resources. Conventional energy sources are becoming increasingly scarce. This phenomenon has been further exacerbated by global population growth. In addition, the exploitation of conventional energy sources has a negative impact on the environment and is changing our planet's climate. It is therefore essential to turn to new energy sources if we want to ensure a sustainable lifestyle for humanity and preserve the environmental balance. The alternative energy source should therefore be respectful of the environment and the human living environment. There is no better candidate than renewable energies. Renewable energy such as photovoltaic energy represents an alternative to this energy deficit. Electricity can be produced using solar cells that convert solar energy. The conversion takes place in the active layer of the cell. Silicon is the material used as the active layer in these solar cells. However, solar cells made from silicon are very expensive. Furthermore, the extraction of silicon damages the environment. It is therefore necessary to use other materials that are less expensive to produce and do not harm the environment, such as perovskites [1,2,3,4]. Perovskites are very easy to handle and therefore easier to integrate into solar cells than silicon. Their use does not pose a significant threat to the environment. The most commonly used perovskites are organic perovskites such as methylammonium lead iodide (MAPI) perovskite [5]. Although this type of perovskite has a good conversion rate, it does have stability issues due to its structure. Inorganic perovskites, on the other hand, have very low conversion efficiency but are more stable than the former.

* Corresponding author: Mona Hermann Charly YAPI

Research on them has increased in recent decades. In this work, we studied the structural, electronic, optical, and elastic properties of $NaSrX_3$ (X: halogen) perovskites [2] using density functional theory (DFT) implemented in Quantum-expresso by GGA [6,7]. We determined the electronic properties of these materials as well as their optical properties.

2. Materials and Methods

2.1. Materials

To perform this work, we used Quantum Expresso (qe-7.0) software, which allows ab initio calculations to be performed [6,7,8]. This software suite ran on Linux Ubuntu 25.04. The Ubuntu 25.04 operating system is installed on a computer with a 2.90 GHz Core i7 processor (Lenovo series). Other programs (besides Quantum Espresso) were also used to process the data generated by Quantum Espresso, namely Vesta, Gnuplot, and Xmgrace. Quantum Espresso itself contains several subprograms designed for very specific tasks.

The materials used are perovskite materials of the $NaSrX_3$ type (X = F and Cl). These materials are assumed to crystallize in a cubic crystal structure (Pm3m). Figure 1 shows a typical representation of the crystal structure of each material.

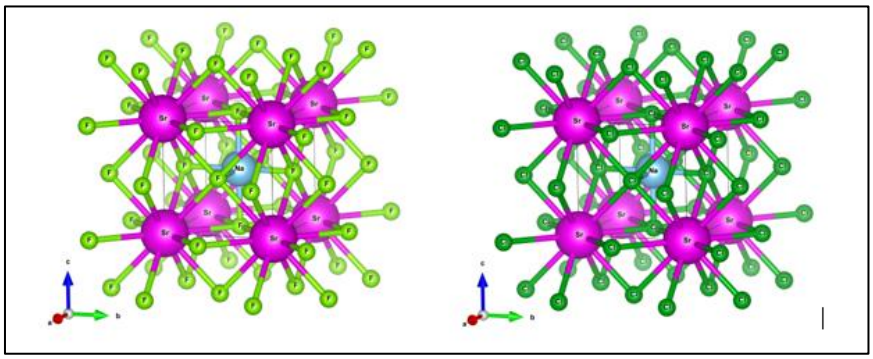

Figure 1 Cubic crystal structure of $NaSrF_3$ (left) and $NaSrCl_3$ (right)

2.2. Methods

This work was carried out using the density functional theory (DFT) method. The density functional theory method is implemented in the Quantum Espresso code [9,10]. Several DFT approximations exist, and we used the generalized gradient approximation (GGA) of Perdew, Burke, and Ernzerhof (PBE + GGA) [11]. The advantage of the GGA method is that it takes into account the local electron density and its first- and second-order gradients included in the enhancement factor. The convergence level of our calculations is set appropriately at 10-9 eV (1.0-9 eV). The kinetic energy cutoff is 80.0 Ry. The k-point grid in the Brillouin zone is 12×12×12. The lattice parameter, kinetic energy cutoff, Monkhorst-Pack k-point sampling in the Brillouin zone, and other structural parameters of cubic perovskite materials of the $NaSrX_3$ type (X = F and Cl) were relaxed to obtain equilibrium parameters.

3. Results and discussion

3.1. Convergence test

Convergence tests were performed on several parameters in order to determine the equilibrium parameters of of cubic perovskite materials of the $NaSrX_3$ type (X = F and Cl). The parameters on which these convergence tests were performed are: the lattice parameter, the cutoff kinetic energy, and the Monkhorst-Pack k-points in the Brillouin zone. The convergence level used is 10^{-10} eV. The convergence test is possible thanks to the vc_relax calculation. To do this, several values of the parameter under consideration are tested by a vc_relax calculation around these parameter values in order to obtain the most stable system. The most stable system corresponds to the parameter value that minimizes the energy of the structure. This value is then chosen as the parameter value to be sought.

3.1.1. Lattice parameter

In the various graphs in Figure 2, we show the evolution of the total energy as a function of the mesh parameter for each structure.

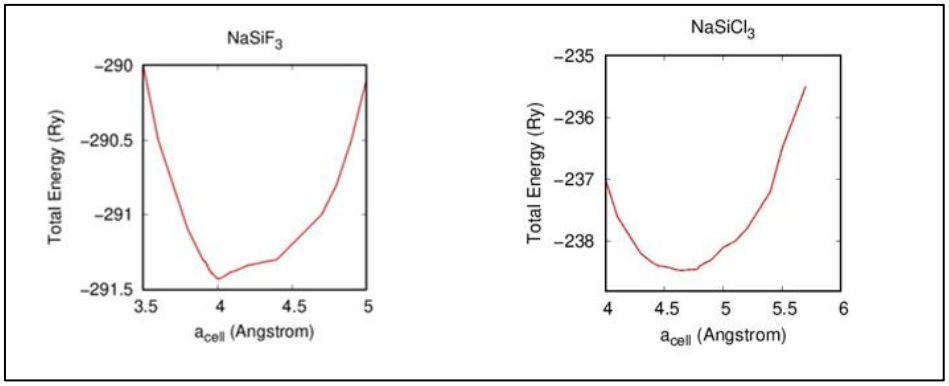

Figure 2 Convergence of Lattice Parameter a_{cell}.

The lattice parameters of the different perovskite materials are shown in Table 1. The lattice parameters obtained are 4.01 Å and 4.65 Å for $NaSrF_3$ and $NaSrCl_3$, respectively. We compared them with those found by M.H. Benkaboua et al [12], Jalil ur Rehman et al [13], Mohammad Reda Kablia et al [14], and Aiman Jehana et al [15]. Our results are lower than those obtained in their papers.

Table 1 Calculated mesh parameters

Latice parameter a_{cell} in Å		
Materials	**Our results**	**Literature results**
$NaSrF_3$	4.01	4.64 [12], 4.78 [13, 14]
$NaSrCl_3$	4.65	5.73 [15]

3.1.2. Convergence of Kinetic energy cut-off

The cutoff kinetic energy (ecut) represents the maximum value of the kinetic energy of the electron wave function in the crystal [16,17,18]. It is the limit that is set in the calculation at each iteration. In our work, the calculation begins to converge at 70 Ry. However, we chose to set this cutoff energy ecut at 80 Ry. It should be noted that the higher the kinetic cutoff energy (ecut), the more accurate the calculations are, which is preferable. However, it should also be noted that a high value for this parameter makes the calculation very complex and therefore very slow. In their work, Jalil ur Rehman et al [13] and Mohammad Reda Kablia et al [14] used 40 Ry for $NaSrF_3$, while Aiman Jehana et al [15] used 60 Ry for $NaSrCl_3$.

3.1.3. Convergence of k-point

We sampled the Brillouin zone of cubic $NaSrX_3$ perovskite structures using the Monkhorst-Pack method [19]. For each structure, convergence is observed from the Monkhorst-Pack points (k_points) 6×6×6. However, we chose to set our Monkhorst-Pack mesh to 12×12×12. This sampling is considered more relevant to the work we have done. The results will be very accurate, but they will be heavier and therefore require more computing time than a 6×6×6 k-point grid. Greater computing resources were therefore necessary. It is worth noting those used by other authors. These include: 17×17×17 for M.H. Benkaboua et al [12], 6×6×6 for Jalil ur Rehman et al [13], 2×2×2 for Mohammad Reda Kablia et al [14], and Aiman Jehana et al [15] did not mention their point_k used.

3.2. Electronic properties

3.2.1. Bands structure

This section presents the different electronic properties of $NaSrX_3$ (X=F and Cl) perovskite materials obtained using the DFT method through GGA formalism. We determined: the electronic band structure, the total density of states (TDOS) and the partial densities of states (PDOS) of cubic $NaSrX_3$ (X= F and Cl) perovskites in the high symmetry directions of the first Brillouin zone. We also determined the band gap energy of $NaSrX_3$ (X= F and Cl) perovskite materials. The magnetic, electronic, optical, and thermal properties of a material depend greatly on its band structure [15]. This is why it is very important to determine the band structure of the material in question in order to study these different properties. The electronic band structures of $NaSrX_3$ perovskite structures (X= F and Cl) are shown in Figure 3. They are calculated in the high-symmetry direction of the first Brillouin zone following the path of high-symmetry points M-Γ-M-R-X-R-M. The electronic band structure of a material is one of the characteristics that differentiates it from other materials. It provides explicit information about the energy values that electrons can have in order to be present in the energy bands. It also indicates the regions where electrons are not available. The valence band (V_B) and the conduction band (C_B) are different energy bands arranged one above the other.

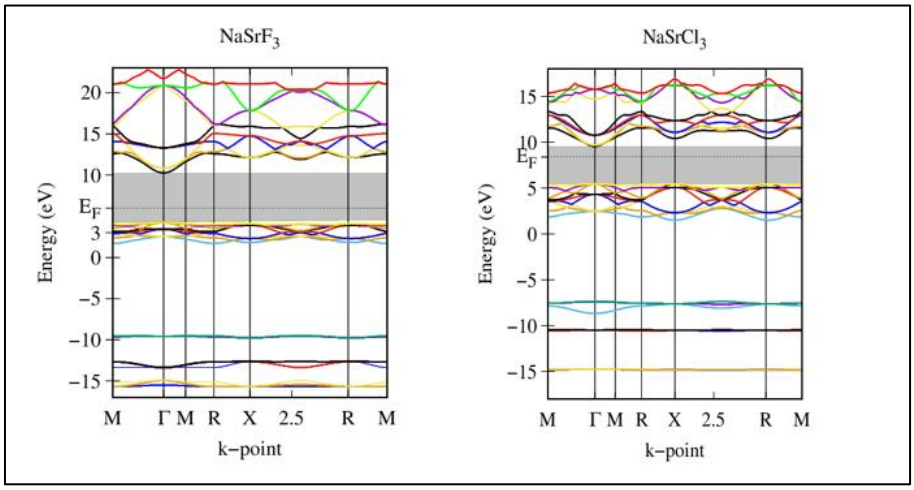

Figure 3 Electronic band structure of $NaSrX_3$ (X= F et Cl)

The valence band is below the Fermi energy level (EF) and the conduction band is above it. The distance between the minimum of the conduction band and the maximum of the valence band is the gap or band gap. This band gap is very important for materials. If it is very wide, the material is an insulator. However, if it is zero, the material is conductive. There is a third type of material with a gap of less than 6 eV, which are semiconductors. The gaps obtained for cubic $NaSrX_3$ (X= F and Cl) perovskite materials are shown in Table 2. We find that $NaSrF_3$ and $NaSrCl_3$ have gaps of 6.02 eV and 4.09 eV, respectively. $NaSrCl_3$ has a very high gap of close to 6 eV. However, it is known that materials with a band gap greater than 5 eV are insulators and those with a gap below 5 eV are semiconductors [20]. We can conclude that $NaSrF_3$ is an insulator, whereas $NaSrCl_3$ is a semiconductor. Other authors have also obtained gap values in their work. For the perovskite $NaSrF_3$, M.J. Mehl et al [21] obtained 5.11 eV and M.H. Benkaboua et al [12] obtained a gap of 4.48 eV, which is significantly lower than ours. For $NaSrCl_3$, Aiman Jehana et al [15] obtained 3.62 eV. The calculated gaps of cubic $NaSrX_3$ (X=F and Cl) perovskite materials are all direct gaps on the Γ-Γ path. These materials are well suited for electronic and optoelectronic applications.

Table 2 Gap values obtained for perovskites $NaSrX_3$ (X= F et Cl**)**

Gap values in eV		
Materials	**Our results**	**Literature results**
$NaSrF_3$	6.02	4.48 [12], 4.78 [13], 5.11 [21]
$NaSrCl_3$	4.09	3.62 [15]

3.2.2. Partial and total densities of state

To understand the contribution of different atomic levels to the density of states (DOS) and the nature of the bonds for these compounds, we determined the total and partial densities of states using the GGA formalism implemented in DFT. The partial density of states for $NaSrX_3$ type perovskite materials (X=F and Cl) are shown in Figure 4. As mentioned for the band structure, here too two bands are very important, namely the conduction band and the valence band.

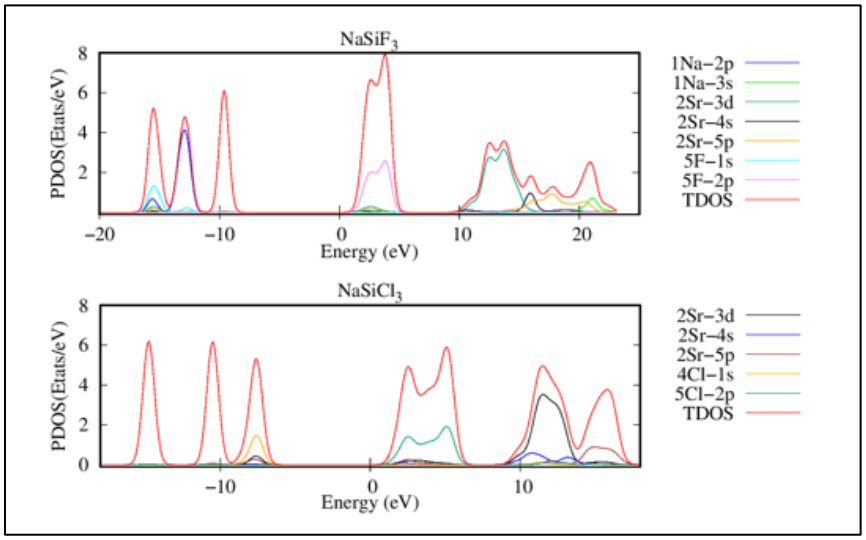

Figure 4 4 Calculated total and partial densities of states for $NaSrF_3$ and $NaSrCl_3$

In $NaSrF_3$ material, the valence band is characterized by the 2p state of F weakly mixed with the 3d state of Sr. The conduction band is characterized by the 3d state of Sr, 4s of Sr, 5p of Sr, and 3s of Na. In this conduction band, the contribution of the 3d state of Sr is very strong. In $NaSrCl_3$ material, the valence band is characterized by the 2p state of Cl weakly mixed with the 3d state of Sr. The conduction band is characterized by the 3d state of Sr weakly mixed with the 4s states of Sr and 5p states of Sr. After this analysis, it appears that the valence bands of $NaSrF_3$ and $NaSrCl_3$ are characterized by the 2p state of the halogen weakly mixed with other states. The bottoms of their conduction bands are all mainly dominated by the 3d states of Sr. These two bands are therefore very important for understanding the properties and applications of these materials.

Now let's look at what happens at the boundaries of the valence band and conduction band of the materials studied. Figure 5 shows these situations. Each figure shows three very important values. These are the maximum valence band (EV), the minimum conduction band (E_C), and the Fermi level (E_F). The Fermi level of each material is well located within the valence band. The Fermi level is closer to the valence band than to the conduction band in $NaSrF_3$. The opposite is true in $NaSrCl_3$. The concentration of free carriers (electrons and holes) is therefore equal. In $NaSrCl_3$, electrons at absolute zero temperature are closer to the conduction band than those in $NaSrF_3$.

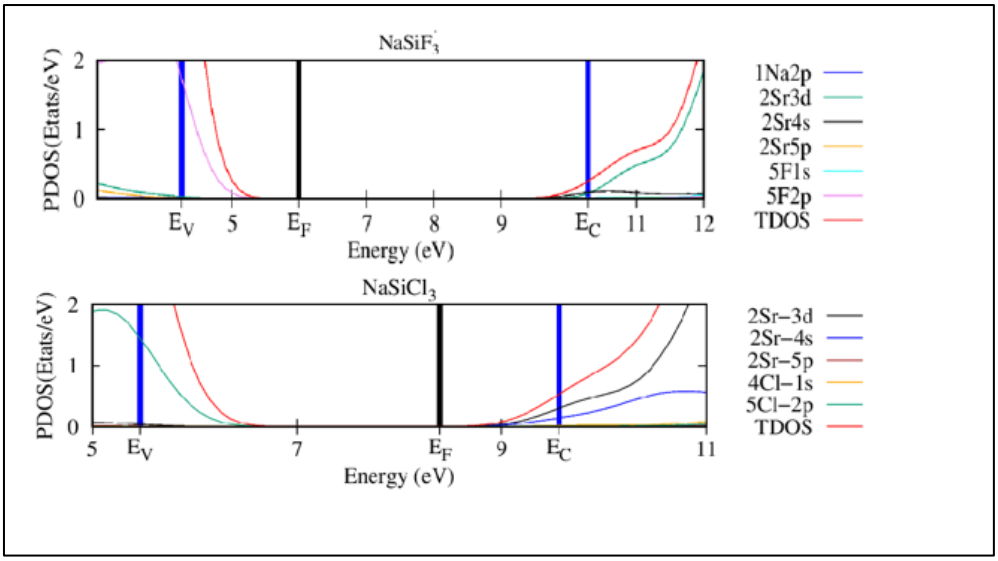

Figure 5 Bands observed at the band gap boundary for $NaSrF_3$ and $NaSrCl_3$

Analysis of each graph shows that there is band overflow in each band gap. These band overflows could lead to a possible reduction in the gap if, for example, doping is carried out. In $NaSrF_3$, it is the 2p states of F and 3d states of Sr that overflow the band gap. In $NaSrCl_3$, the band overflows are due to the 2p states of Cl, 3d states of Sr, and 4s states of Sr.

We have represented in Figures 6 and 7 the charge densities of the two compounds in the (110) and (100) crystallographic planes, respectively, to better understand the nature of the bond between the different atoms contained therein.

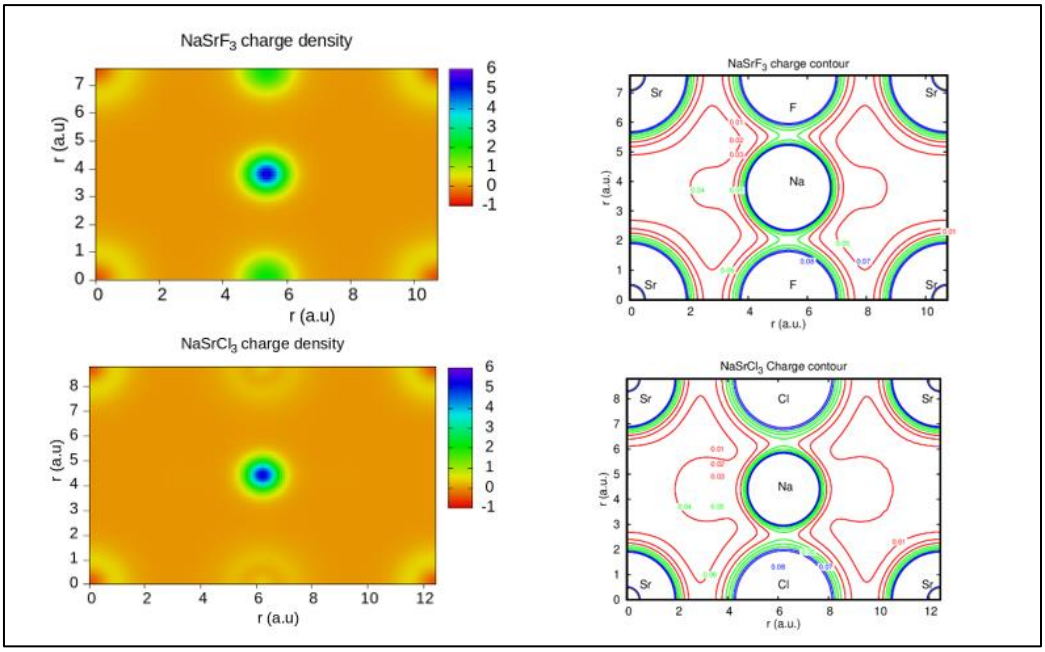

Figure 6 Charge denssity of $NaSrF_3$ and $NaSrCl_3$ in crystallographic plane (110)

The binding and charge distribution behavior between atoms can be understood using the valence electron charge density derived from convergent wave functions. The valence electron charge densities are calculated for the (110) crystallographic plane and the results obtained for $NaSrF_3$ and $NaSrCl_3$ are summarized in figure 6.

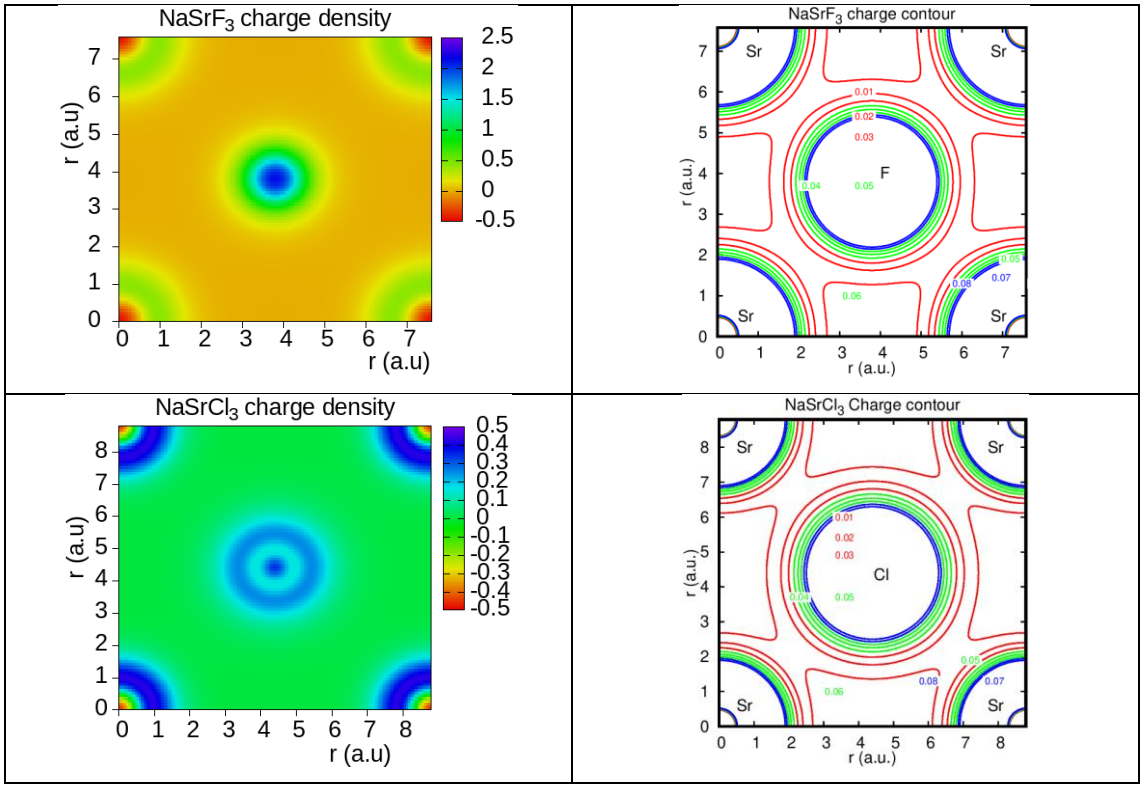

Figure 7 Charge denssity of $NaSrF_3$ and $NaSrCl_3$ in crystallographic plane (100)

The charge density graphs show a maximum density near the fluorine and chlorine atom, certainly due to their high electronegativity compared to the other atoms present in these perovskites. We also notice that the charge distribution is almost identical in these two compounds. The charge distribution is strongly localized around the center of halogen atoms. The charge density map of these compounds assumes an ionic bond or a metal bond between these atoms. It should be remembered that to our knowledge no author has discussed the charge density of these compounds.

3.3. Optical properties

3.3.1. Real part and imaginary part of the complex dielectric function

To design electronic and optoelectronic devices using materials, it is necessary to understand how these materials interact with light. It is therefore necessary to study their optical properties. If their optical properties are known, their future applications can be predicted. The optical characteristics sought in a material are: low refractive index, high absorption coefficient in a certain wavelength range, etc. To achieve this, the optical parameters of the material must be correctly estimated. This will enable the emergence of innovative electronic components. The dielectric function is the basic quantity for determining the optical properties of any material. The complex dielectric function $\tilde{\varepsilon}$ is the response of the electrons in a compound when it receives electromagnetic radiation. It is written as : $\tilde{\varepsilon}(\omega) = \varepsilon_r(\omega) + i\varepsilon_i(\omega)$, where ε_r and ε_i are the real part and the imaginary part, respectively. They are obtained using the Kramers Kronig relation [22]. The imaginary part ε_i is responsible for the absorption of the material, while the real part ε_r is related to the polarization of the medium. In our work, the real and imaginary parts of the complex dielectric function of $NaSrF_3$ and $NaSrCl_3$ perovskites are shown in figure 8. All these curves have two very significant parts. The first part ranges from 0 eV to 10 eV and the second from 20 eV to 30 eV. The first part is characterized by various fluctuations. These fluctuations are more or less significant. The second part also includes fluctuations, but they are less significant than the previous ones. The maximum peak of the real part of the dielectric function of the $NaSrF_3$ and $NaSrCl_3$ compounds are positioned at energies of 6.24 eV and 5.44 eV, respectively. As for the imaginary part of the dielectric function of the $NaSrF_3$ and $NaSrCl_3$ compounds, they are located at energies of 8.24 eV and 5.84 eV, respectively.

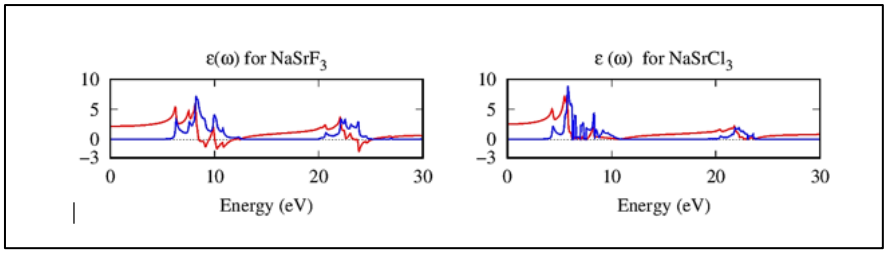

Figure 8 Real part (red) and imaginary part (blue) of the dielectric function calculated

3.3.2. Optical functions

The dielectric function is used to deduce optical functions such as: the refractive index n(ω), the extinction coefficient k(ω), the reflection coefficient or reflectivity R(ω), the absorption coefficient α(ω), and the optical conductivity σ(ω).

Refractive index n(ω)

The complex refractive index helps us understand how photons affect the medium as they propagate [22]. It has two significant parts: the real part and the imaginary part. The real part is the real refractive index n(ω), which describes the phase velocity of the incident wave. The imaginary part is the extinction coefficient k(ω). It represents the reduction in incident light. When the real refractive index of the medium is high, the wave travels more slowly and is therefore more likely to be deflected. If the imaginary part is non-zero, the medium absorbs light at the wavelength at which it is non-zero. This wave then weakens more and more as it propagates. A transparent material has a zero imaginary part and a non-zero, positive real part. Figure 9 shows the refractive index of $NaSrF_3$ and $NaSrCl_3$.

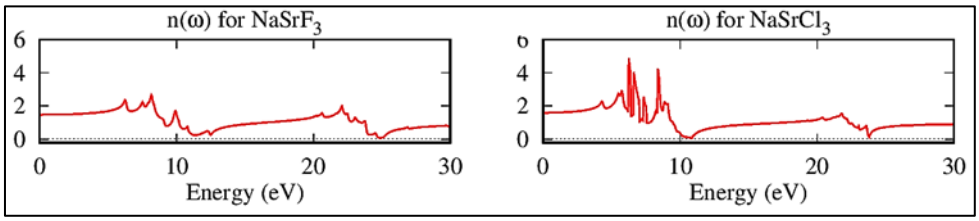

Figure 9 Refractive index for $NaSrX_3$ halide perovskites (X = F and Cl)

Each compound studied has a positive refractive index. The refractive index is zero and is high at certain points. We can therefore say that light passing through these materials is likely to be slower and more deflected in the visible and UV ranges. $NaSrF_3$ and $NaSrCl_3$ have main peaks of 2.63 to 8.15 eV and 2.89 to 5.76 eV, respectively. However, Jalil ur Rehman [13], in their work, obtained a main peak for $NaSrF_3$ at 9.36 eV. Mohammad Reda Kabli et al obtained a maximum peak of 1.50 to 9.53 eV [14]. For $NaSrCl_3$, Aiman Jehan et al obtained 2.1 to 6.6 eV [15]. Our refractive indices at frequency 0, i.e., n(0), are 1.47 and 1.59 for $NaSrF_3$ and $NaSrCl_3$, respectively. Aiman Jehan et al. obtained 1.5 for $NaSrCl_3$ [15]. M.H. Benkabou et al obtained 1.4 for $NaSrF_3$ [12].

Extinction coefficient K(ω)

Figure 10 shows the extinction coefficient K(ω) for each calculated perovskite material $NaSrF_3$ and $NaSrCl_3$. The main peaks in the $NaSrF_3$ and $NaSrCl_3$ materials are 1.69 to 8.44 eV and 1.74 to 5.84 eV, respectively. From 3.85 eV to 15 eV and from 18.5 eV to 31 eV, the extinction coefficient K is non-zero in both materials. It should be noted that for these energy ranges, these materials absorb the light they receive. The wave will therefore weaken more and more as it propagates. On the other hand, in the energy regions where the extinction coefficient is zero, these materials will be transparent, which is confirmed by the non-zero value of the refractive index in these regions. We can therefore deduce that $NaSrF_3$ and $NaSrCl_3$ are transparent from 0 to 4 eV and from 0 to 3 eV, respectively. No author has discussed the extinction coefficient in the literature for $NaSrF_3$ and $NaSrCl_3$.

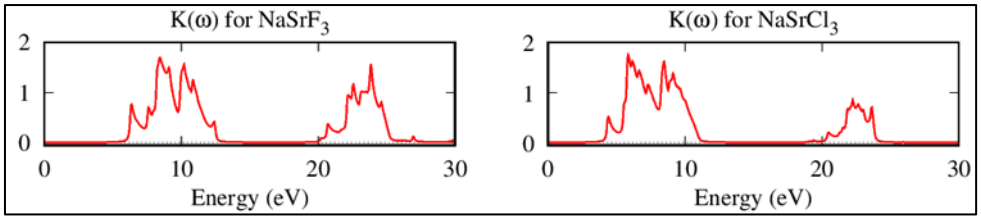

Figure 10 Extinction coefficient for $NaSrX_3$ halide perovskites (X = F and Cl)

Reflexivity R(ω)

Figure 11 shows the calculated optical reflectivity R(ω) of the perovskites $NaSrF_3$ and $NaSrCl_3$. Optical reflectivity describes the ability of a surface to reflect light. It represents the ratio of the reflected light intensity to the incident light intensity. High reflection peaks are observed at energies of 6.30 eV, 9.13 eV, 10.30 eV, 11.74 eV, 12.51 eV, 24.00 eV, and 24.85 eV for $NaSrF_3$, and 5.80 eV, 8.39 eV, 10.95 eV, and 23.85 eV for $NaSrCl_3$. The reflection coefficient values in $NaSrF_3$ are lower than those observed in $NaSrCl_3$. M.H. Benkabou et al obtained peaks at 10.78 eV, 25.02 eV, and 28.94 eV for $NaSrF_3$ [12]. Jalil ur Rehman et al obtained their main peak at 6.03 eV [15]. At zero frequency, the reflectivity values observed are 0.036 and 0.037 for $NaSrF_3$ and $NaSrCl_3$, respectively.

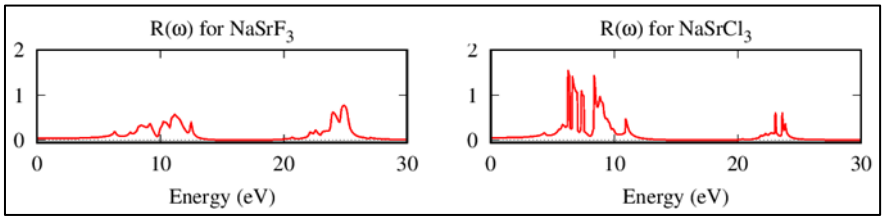

Figure 11 Reflexivity for $NaSrX_3$ halide perovskites (X = F and Cl)

Absorption coefficient α(ω)

Figure 12 shows the absorption coefficient α(ω) calculated for the perovskites $NaSrF_3$ and $NaSrCl_3$. The optical absorption coefficient reflects the decrease in the intensity of light radiation as it passes through a material. The material strongly absorbs light if the absorption coefficient is high. It then converts it into thermal energy. This results in low transmission or reflection. If the absorption coefficient is low, the material has high transparency. The absorption coefficient also reveals the metallic, semiconductor, or insulating nature of the material. In our work, the absorption of both materials starts at 2.82 eV. The curves show two coinciding energy absorption zones. These are 2.82 eV to 13.78 eV and 18.40 eV to 30 eV. The main absorption peak for each material is in the first part. It is 5.9 eV for $NaSrF_3$ and 8.44 eV for $NaSrCl_3$.

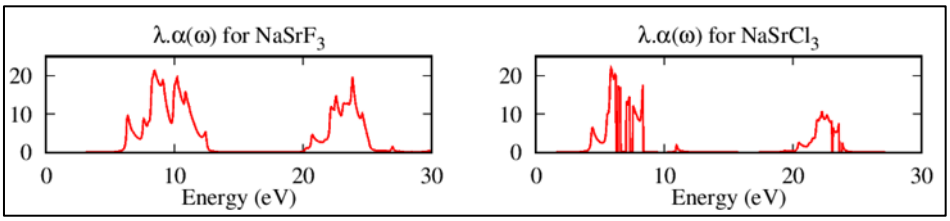

Figure 12 Absorption coefficient for $NaSrX_3$ halide perovskites (X = F and Cl)

Optical conductivity σ(ω)

Figure 13 shows the optical conductivity σ(ω) calculated for $NaSrF_3$ and $NaSrCl_3$. The transport of electrons when the material reacts to incident light is explained by the optical conductivity σ(ω) [23]. For each compound, σ(ω) initially behaves as almost zero, then increases. The imaginary value of the conductivity (real part) at 0 eV is zero for $NaSrF_3$ and $NaSrCl_3$. The imaginary value of the conductivity is not zero for $NaSrF_3$ and $NaSrCl_3$ at 0 eV. This function then adopts more or less decreasing fluctuations as the energy increases. The main peak of conductivity (real) for $NaSrF_3$ is located at 8.41 eV and 5.80 eV for $NaSrCl_3$. The main peak of conductivity (imaginary) for $NaSrF_3$ appears at 23.87 eV, while that of $NaSrCl_3$ appears at 10.87 eV.

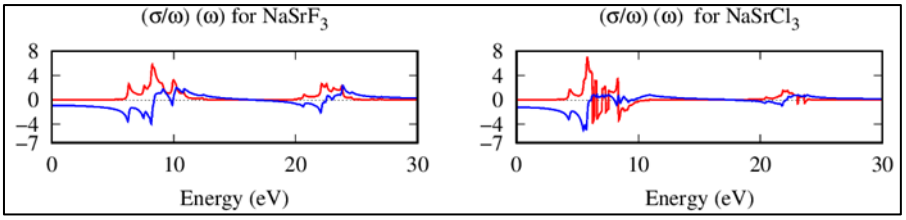

Figure 13 Optical conductivity for $NaSrX_3$ (real part in blue and imaginary part in red**)**

Energy loss function L(ω)

The energy loss spectrum L(ω) depends on the dielectric function $\tilde{\varepsilon}(\omega)$, and therefore on the frequency ω of the external electric field [22]. L(ω) is useful for understanding the collective excitation spectra produced by an electron passing through a material. The peak in the L(ω) spectra appears at a particular frequency or energy of the incident light. This is the plasma frequency. Figure 14 shows the energy loss spectrum for each compound. Since the observed energy region is less than 50 eV, L(ω) corresponds to the valence loss spectrum. This energy region corresponds to the dielectric response for frequencies ω of 10^3 GHz. In this region, valence electrons cause resonant oscillations. When the value of $\varepsilon_i(\omega)$ is very low and $\varepsilon_r(\omega)$ is zero or close to zero, the loss function shows a sharp peak [22]. The frequency at which this occurs is the plasma frequency ω_P, and the corresponding energy is $E = \hbar\omega_P$.

The maximum resonant energy loss is equal to 19.75 u.a. at 25.22 eV and 15.73 u.a. at 10.92 eV for $NaSrF_3$ and $NaSrCl_3$, respectively. Another secondary peak appears in each material and is in the opposite position in each case : in $NaSrF_3$, it is located before the largest peak, and in $NaSrCl_3$, after the largest peak. They are positioned at 12.52 eV and 23.84 eV for $NaSrF_3$ and $NaSrCl_3$, respectively. According to other studies, the maximum energy loss is equal to 1.44 at 24.70 eV [14] and 26.15 eV [13] for $NaSrF_3$. We found nothing in the literature for $NaSrCl_3$.

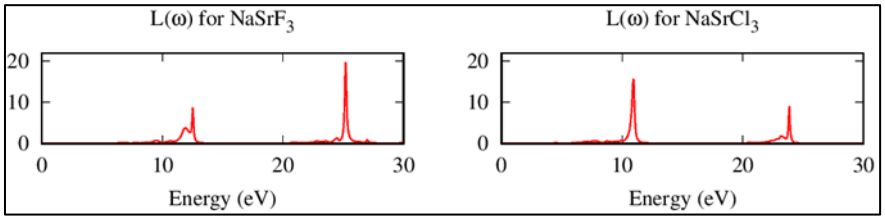

Figure 14 Energy loss function spectrum

3.4. Elastic properties

Elastic properties provide useful information about the mechanical and dynamic behavior of the material, its anisotropy, stiffness, ductility or brittleness, etc. These elastic properties are described by independent elastic parameters. For cubic symmetry, three elastic constants are needed to characterize the material elastically. These are: C_{11}, C_{12}, and C_{44}. Each represents the directional mechanical responses of the crystal for different directions of forces or stresses applied to these materials [24,25].

Elastic constants

The parameters C_{11}, C_{12}, and C_{44} calculated for the inorganic halogenated perovskite materials $NaSrF_3$ and $NaSrCl_3$ are shown in Table 3.

Table 3 Elastic parameters and mechanical stability criteria of cubic crystals $NaSrX_3$ (F and Cl)

	C_{11} (GPa)	C_{12} (GPa)	C_{44} (GPa)	$C_{11}+2C_{12}$ (GPa)	$C_{11}-C_{12}$ (GPa)	$\frac{C_{11}}{C_{12}}$	$\frac{C_{11}}{C_{44}}$
$NaSrF_3$	34.90	25.69	16.17	86.29	9.21	1.35	2.15
$NaSrCl_3$	90.63	34.65	47.55	159.94	55.98	2.61	1.90

Where we obtained C_{11}, C_{12}, and C_{44}, values of 34.90 GPa, 25.69 GPa, and 16.17 GPa for $NaSrF_3$, M.H. Benkabou et al obtained results of 43.90 GPa, −5.75 GPa, and 2.75 GPa for C_{11}, C_{12}, and C_{44}, respectively [12]. With $NaSrCl_3$, we obtained 90.63 GPa, 34.65 GPa, and 47.55 GPa for C_{11}, C_{12}, and C_{44}, respectively. Aiman Jehan et al. obtained 54.38 GPa, -0.169 GPa, and 4.94 GPa for C_{11}, C_{12}, and C_{44}, respectively [15]. C_{11} reflects unidirectional compression along the crystallographic directions [25,26]. Since C_{11} is higher than C_{12} and C_{44} in both materials, there is therefore lower resistance to pure shear deformation compared to unidirectional compression resistance. The elastic constants satisfy the mechanical stability criteria for cubic crystals [26] : $C_{11} > 0$; $C_{44} > 0$; $C_{11} - C_{12} > 0$; $C_{11} + 2C_{12} > 0$

Differents mechanical parameters.

Other parameters related to elastic properties are determined using elastic constants. Table 4 shows the elastic anisotropy factor A, the modulus of elasticity B, Cauchy pressure C_P, Young's modulus E, Reuss shear moduli (Gr), Voigt shear moduli (G_V), Shear modulus (G), Poisson's ratio (σ), Kleinman parameter (**ζ**), Pugh's ratio (B/G), P-Wave modulus P_W, Shear constant Cs, Lamé constant (λ et μ), compressibility (β) et Melting Temperature T_m of $NaSrX_3$ perovskites that we have calculated.

Table 4 Calculated other mechanical parameters for cubic $NaSrX_3$ (F and Cl) perovskites

Parameters	**Symbol**	**$NaSrF_3$**	**$NaSrCl_3$**
Elastic constants	C_{11} (GPa)	34.90 43.90 [13]	90.63 54.38[15]
	C_{12} (GPa)	25.69 −5.75 [13]	34.65 -0.169[15]
	C_{44} (GPa)	16.17 2.75 [13]	47.55 4.22[15]
mechanical stability criteria	$C_{11} + 2C_{12}$ (GPa)	86.29	159.94
	$C_{11} - C_{12}$ (GPa)	9.21	55.98
	$\frac{C_{11}}{C_{12}}$	1.35	2.61
	$\frac{C_{11}}{C_{44}}$	2.15	1.90
Anisotropy factor	A	1.66 0.305 [13]	1.43 0.47[15]
Voigt bulk moduli	B_V	20.20	41.76
Voigt shear moduli	Gv (GPa)	21.83	53.59
Reuss shear moduli	Gr (GPa)	8.07	37.16
Shear modulus	G (GPa)	14.95 7.92 [13]	45.38 17.47[15]
Bulk modulus	B (GPa)	28.76 10.8 [13]	53.31 20.59[15]
Cauchy pressure	C_P (GPa)	9.51	-12.89
Young's modulus	E (GPa)	38.22 19.1 [13]	106.04 40.80[15]
Shear constant	C_S (GPa)	04.61	27.99
Poisson's ratio	σ	0.28 0.28 [13]	0.17 0.169[15]
Kleinman parameter	ζ(GPa)	0.81	0.52
Pugh's ratio	$\frac{B}{G}$	1.92 1.36 [13]	1.17 1.17[15]
Hardness	Hv (GPa)	2.21	10.03
Compressibility	β	0.03	0.02
P-Wave modulus	P_W(GPa)	20.51	77.42
Lamé constant	λ (GPa)	18.80	23.06
Lamé constant	μ (GPa)	14.95	45.38

Melting Temperature	T_m ± 300 (K)	760.33	1089.74

The compressibility modulus (B) provides information about the stability of a material. It is considered stable if B satisfies the condition $C_{12} < B < C_{11}$ [25,26]. The values of B calculated for $NaSrX_3$ perovskite materials satisfy this latter condition. They can therefore be considered stable. An isotropic material has an anisotropy factor A equal to 1. For anisotropy, this factor is different from 1. The values of A found in this work are greater than 1. These compounds are therefore anisotropic. The stiffness of a material is evaluated by Young's modulus (E). The higher it is, the more rigid the material is. But when it is low, the material is less rigid. The different values of E calculated allow us to conclude that all these perovskites have very good rigidity. The Pugh $\frac{B}{G}$ ratio can be used to quantitatively estimate whether the material behaves in a brittle or ductile manner [27]. The ductile or brittle nature of the material is separated by a critical value of 1.75 [27]. If $\frac{B}{G}$ is greater than 1.75, the material is ductile, but if $\frac{B}{G}$ is less than 1.75, the material is brittle. In this work, NaSrF3 has a $\frac{B}{G}$ value greater than 1.75, while NaSrCl3 has a $\frac{B}{G}$ value less than 1.75. NaSrF3 is therefore ductile and NaSrCl3 is brittle. The Poisson's ratio σ deals with the characteristics of bond forces [28]. It is always less than 0.50. For ionic materials, the expected σ value is 0.25 [28]. For covalent materials, we must have $\sigma < 0.1$. Ductile materials usually have a high Poisson's ratio ($\sigma > 0{,}26$). The value σ is 0.28 for the material $NaSrF_3$ and 0.17 for $NaSrCl_3$. Kleinman's parameter ζ quantifies internal stress [29]. It indicates the relative ease of bending the bond versus stretching the bond. In a system, when ζ=0, the bending of the bond is minimized; however, when ζ=1, the stretching of the bond is minimized. The values of ζ found for $NaSrF_3$ and $NaSrCl_3$ perovskites are 0.81 and 0.52, respectively, which are close to 1. We assume that these materials show greater resistance to bond bending and bond angle distortion. In addition, these perovskite materials exhibit lower resistance to pure shear deformation compared to unidirectional compression. Hardness is necessary to understand the elastic and plastic properties of a compound. The hardness obtained is 2.21 GPa and 10.03 GPa for $NaSrF_3$ and $NaSrCl_3$, respectively. The PW wave modulus measures a material's ability to resist compression and elongation in the direction of mechanical wave propagation. The higher the PW, the more rigid the material. This means that additional force will be required to deform the material [30, 31]. Our P_W values are 20.51 GPa and 77.42 GPa for $NaSrF_3$ and $NaSrCl_3$, respectively. At the melting temperature, the solid and liquid phases coexist in equilibrium at a given pressure. This thermodynamic characteristic of a material indicates the applicable upper temperature limit [32]. The melting temperature (T_m) of $NaSrF_3$ is 760.33 K and that of $NaSrCl_3$ is 1089.74 K. $NaSrCl_3$ will withstand higher temperatures than $NaSrF_3$.

4. Conclusion

The structural, electronic, optical, and elastic properties of $NaSrX_3$ (X=F and Cl) perovskite materials were studied using the DFT method with the GGA approximation. The lattice parameter calculated for $NaSrF_3$ and $NaSrCl_3$ is 4.01 Å and 4.65 Å, respectively. The electronic band structure showed respective gaps of 6.02 eV and 4.09 eV. $NaSrF_3$ exhibits insulating behavior and $NaSrCl_3$ exhibits semiconducting behavior. Both have direct gaps on the Γ-Γ path of the Brillouin zone. These materials are potential optoelectronic devices. The band overlap in the band gap presented by the density of states shows that $NaSrF_3$ can be semiconducting through doping. Regarding optical properties, the refractive index shows that the materials are capable of slowing down light and deflecting it in the visible and UV range. Analysis of the extinction coefficient shows that these materials absorb light in the range from 2.25 eV to 15 eV and from 18.5 eV to 31 eV. They will be transparent in other energy ranges.

The reflection coefficient values observed for $NaSrF_3$ are lower than those observed for $NaSrCl_3$. These materials strongly absorb light in the UV range. The elastic parameters for $NaSrF_3$ and $NaSrCl_3$ are reported. The calculated elastic constants meet the criteria for mechanical stability. $NaSrF_3$ is ductile and $NaSrCl_3$ is brittle according to Pugh's criteria. Both are ionic and show greater resistance to bond bending and bond angle distortion. The melting temperature (Tm) of $NaSrF_3$ is higher than that of $NaSrCl_3$. $NaSrCl_3$ will be more resistant to high temperatures than $NaSrF_3$. This work confirms that the compounds $NaSrF_3$ and $NaSrCl_3$ are of great interest as optoelectronic devices. They have very good elastic and optical properties. $NaSrCl_3$ has very good semiconductor properties that could be exploited for the development of various applications. $NaSrF_3$, even though it has insulating properties, can be doped with impurities or even integrated as an insulator in electronic devices.

Compliance with ethical standards

Acknowledgments

We would like to thank the Physics Department at Jean Lorougnon Guédé University (UJLoG) in Daloa and the Fundamental and Applied Physics Laboratory (LPFA) at Nangui Abrogoua University (Abidjan, Ivory Coast) for their collaboration in this study.

Disclosure of conflict of interest

The authors declare that there are no conflicts of interest that is relevant to the content of this article.

References

[1] G Ajay, M S Sirajuddeen, A Venkatesan. First-principles investigation of structural, electronic, and optical properties of cubic halide perovskite RbSrI3. December 2023. Chemical Physics Impact 8:100431. DOI:10.1016/j.chphi.

[2] M Ullah, N Ullah, A M Tighezza, B Bashir, K Batool & G H Murtaza. Bandgap Nature Transition and the Optical Properties of ABX_3(A = K, Rb; B = Sr, Ba, Ca; X = Cl, Br, I) Perovskites under Pressure. Journal of Inorganic and Organometallic Polymers and Materials. 07 August 2024.

[3] L Chouhan, S Ghimire, C Subrahmanyam, T Miyasaka and V Biju. Synthesis, optoelectronic properties and applications of halide perovskites. Chem Soc Rev. 2020. 49(10), DOI: 10.1039/C9CS00848A.

[4] R K Pingak1, S Bouhmaidi, L Setti, B Pasangka, B Bernandus, H I Sutaji, F Nitti and M Z Ndii. Structural, Electronic, Elastic, and Optical Properties of Cubic $BaLiX_3$(X = F, Cl, Br, or I) Perovskites: An Ab-initio DFT Study. Indones. J Chem. 2023. 23 (3). 843 - 862

[5] T Hellmann, Chittaranjan D, T Abzieher, J A Schwenzer, M Wussler, R Dachauer, U W Paetzold, W Jaegermann, and T Mayer. The electronic structure of mapi-based perovskite solar cells: Detailed band diagram determination by photoemission spectroscopy comparing classical and inverted device stacks. Advanced Energy Materials. 10(42):2002129. Nov 2020.

[6] P Giannozzi, O Andreussi, T Brumme, O. Bunau, M. Buongiorno Nardelli, M. Calandra, R Car, C Cavazzoni, D Ceresoli, M Cococcioni, N Colonna, I Carnimeo, A Dal Corso, S de Gironcoli, P Delugas, R A DiStasio Jr, A Ferretti, A Floris, G Fratesi, G Fugallo, R Gebauer, U Gerstmann, F Giustino, T Gorni, J Jia, M Kawamura, H-Y Ko, A Kokalj, E Küçükbenli, M Lazzeri, M Marsili, N Marzari, F Mauri, N L Nguyen; H-V Nguyen, A Otero-de-la-Roza, L Paulatto, S Poncé, D Rocca, R Sabatini, B Santra, M Schlipf, A P Seitsonen, A Smogunov, I Timrov, T Thonhauser, P Umari, N Vast, X Wu & S Baroni (2017). "Advancd capabilities for materials modelling with Quantum ESPRESSO".

[7] P Giannozzi, S Baroni, N Bonini, M Calandra, R Car, C Cavazzoni, D Ceresoli, G L Chiarotti, M Cococcioni, I Dabo, A Dal Corso, S Fabris, G Fratesi, S de Gironcoli, R Gebauer, U Gerstmann, C Gougoussis, A Kokalj, M Lazzeri, L Martin-Samos, N Marzari, F Mauri, R Mazzarello, S Paolini, A Pasquarello, L Paulatto, C Sbraccia, S Scandolo, G Sclauzero, A P Seitsonen, A Smogunov, P Umari, and R M Wentzcovitch. QUANTUM ESPRESSO: a modular and open-source software project for quantum simulations of materials. Journal of Physics: Condensed Matter. (2009), 21(39), p. 395502.

[8] A M Rappe, K M Rabe, E Kaxiras and J D Joannopoulos. Optimized pseudopotentials. Phys. Rev. B 44, (1991), 13175.

[9] J P Perdew, K Burke, K and M G Ernzerhof. Generalized Gradient Approximation Made Simple. Phys Rev Lett. 77(1996)3865 and Phys Rev Lett. 78(1997)1396.

[10] A D Becke. Density-functional exchange-energy approximation with correct asymptotic behavior. In: Physical Review A, (1988), 38(6), p. 3098–3100.

[11] J P Perdew, K Burke & M Ernzerhof. Generalized Gradient Approximation Made Simple. [Phys. Rev. Lett. 77, 3865 (1996)]. In: Physical Review Letters, (1997), 78(7), p. 1396-1396.

[12] M H Benkabou, M Harmela, A Haddoua, A Yakoubia, N Bakia, R Ahmedb, Y Al-Douric, S V Syrotyuke, H Khachaia, R Khenataf, C H Voong, M.R Johanc. Structural, electronic, optical and thermodynamic investigations of $NaXF_3$(X=Ca and Sr): First-principles calculations. Chinese Journal of Physics. 56(2018)131-144.

[13] Jalil ur Rehman, N Ahmad, M Usman, H Alrobei, M B Tahir, Khurram Shahzad, Abid Hussain, M Awais Rehman, Arshid Mahmood Ali, Shabbir Muhammad. First-principles calculations to investigate structural, electronic and optical properties of Na based fluoroperovskites $NaXF_3$ (X= Sr, Zn). Solid State Communications 334–335(2021)114396.

[14] Mohammad Reda Kablia, Jalil ur R, M B Tahirb, M Usmanb, A M Alic, K Shahzadd. Structural, electronics and optical properties of sodium based fluoroperovskites $NaXF_3$ (X = Ca, Mg, Sr and Zn): First principles calculations. Physics Letters A 412 (2021) 127574.

[15] Aiman Jehan, M Husain, N Sfinac, S N Khana, N Rahman, V Tirthe, R Khand, M Sohaild, A A Rachedg, A Khana. First-principles calculations to investigate structural, elastic, electronic, and optical properties of $XSrCl_3$(X =Li, Na). Optik-International Journal for Lightand Electron Optics 287(2023)171088.

[16] Md Tanvir Hossain, F-T Zahr, R A-A Dhroobo, Md M Hasan, Md R Al Amin, F M A Sieam, S Swargo, S T Disha, R Islam. First-principles insights into the structural, mechanical, electronic, optical, and thermophysical properties of $XSrBr_3$(X = Na, Ga, and Tl) perovskites: Implications for optoelectronic applications. Materials Science in Semiconductor Processing 182 (2024) 10869.

[17] Md Tanvir Hossain, Tasmi A, Jahirul I, Md Al-A B Shuvo a, K Hossain, Md A Hossain. Investigation of structural, mechanical, electronic, optical, and thermodynamic properties of AXI_3(A = Li, Na; X = Ca, Sr, and Ba) halide perovskites for emerging energy technologies: A DFT study; Materials Science in Semiconductor Processing. Volume 188. 2025. 109235.

[18] Sapkota, Dhruba. Study of structural and electronic properties of sodium and potassium. Diss. Department of Physics Birendra Multiple Campus, 2020.

[19] H J Monkhorst and J D Pack. Special Points for Brillouin-Zone Integrations. Physical Review B. (1976). Vol 13. pp 5188-5192.

[20] Dian Dwiriani, M Z Efendi, R Aritonang, T U Lestari. Band gap energy characteristics in materials. Journal of frontier research in science and engineering. 3(2)(2025).

[21] M J Mehl. Pressure dependence of the elastic moduli in aluminum-rich Al-Li compounds. Phys Rev B 47 (1993) 2493–2500.

[22] J Islam, K Hossain. First-principles simulations to investigate effect of hydrostatic pressure on structural, mechanical, electronic, and optical properties of the $AgCdCl_3$ perovskite. Emergent Mater 6 (2023) 1763–1777. https://doi.org/ 10.1007/s42247-023-00565-1.

[23] A Darvishzadeh, N Alharbi, A Mosavi, N E Gorji. Modeling the strain impact on refractive index and optical transmission rate. Phys B Condens. Matter 543 (2018) 14–17. https://doi.org/10.1016/j.physb.2018.05.001.

[24] Jérôme Lelièvre. New lead-free materials based on bismuth: towards lead-like compounds (A,A')(B)O_3 et (A,A')(BB')O_3. University doctoral thesis. Specialty: Ceramic materials and surface treatments. University of Limoges, France. 2017. 210 p.

[25] M Houari, B Bouadjemi, M Matougui, S Haid, T Lantri, Z Aziz, S Bentata and B Bouhafs. Optoelectronic properties of germanium iodide perovskites $AGeI_3$ (A= K, Rb and Cs): 1st principles investigations. In : Springer Nature. (2019). Vol. 51. No. 7. p 1–14.

[26] M Houari, B Bouadjemi, S Haid, M Matougui, T Lantri and Z Aziz. Semiconductor behavior of halide perovskites $AGeX_3$ (A = K, Rb, Cs; X = F, Cl Br): first-principles calculations. Indian J Phys. (2019). Vol. 97. pp 1-13.

[27] S F Pugh. Relations between the elastic moduli and the plastic properties of polycrystalline pure metals. The London Edinburgh and Dublin Philosophical Magazine and Journal of Science. (1954). Vol 45. No 367. pp 823–843.

[28] Amel Meziani. Study of the structural, electronic, elastic, and optical properties of the fluoro-perovskite compounds $CsCdF_3$ and $KZnF_3$. University doctoral thesis, Specialization: Condensed matter physics. Mokhtar Badj University, Algeria. 2012. 95 p.

[29] B Kleinman, M Karplus; Phys Rev. B 3 (1971) 24.

[30] S Chibani, O Arbouche, M Zemouli, Y Benallou, K Amara, N Chami, M Ameri, M E Keurti. First-principles investigation of structural, mechanical, electronic, and thermoelectric properties of Half-Heusler compounds RuVX (X=As, P, and Sb). Comput Condens Matter 16. (2018) e00312. https://doi.org/10.1016/j.

[31] Mavko G, Mukerji T, and Dvorkin J. (1998) The Rock Physics Handbook: Tools for Seismic Analysis in Porous Media. Cambridge University Press, 208-210.

[32] Q Fan, C Chai, Q Wei, H Yan, Y Zhao, Y Yang, X Yu, Y Liu, M Xing, J Zhang, R Yao. Novel silicon allotropes: stability, mechanical, and electronic properties. J Appl Phys. 118 (2015) 185704, https://doi.org/10.1063/1.4935549.